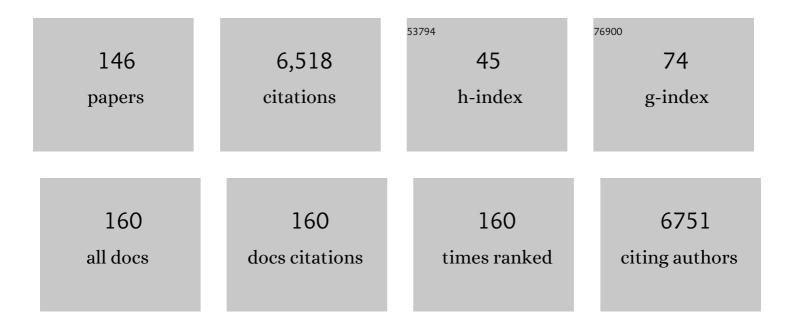
## Lei Zhu

## List of Publications by Year in descending order

Source: https://exaly.com/author-pdf/1898463/publications.pdf Version: 2024-02-01



1 = 7 - 1 - 1

#	Article	IF	CITATIONS
1	Controllable Preparation of Chiral Oxazoline-Cu(II) Catalyst as Nanoreactor for Highly Asymmetric Henry Reaction in Water. Catalysis Letters, 2022, 152, 106-115.	2.6	3
2	Triple Emission of 5′-(para-R-Phenylene)vinylene-2-(2′-hydroxyphenyl)benzoxazole (PVHBO). Part II: Emission from Anions. Journal of Physical Chemistry A, 2022, , .	2.5	2
3	Triple Emission of 5′-( <i>para</i> -R-Phenylene)vinylene-2-(2′-hydroxyphenyl)benzoxazole (PVHBO). Part I: Dual Emission from the Neutral Species. Journal of Physical Chemistry A, 2022, 126, 1033-1061.	2.5	7
4	Palladium-Catalyzed Intramolecular Diarylation of 1,3-Diketone in Total Synthesis of (±)-Spiroaxillarone A. Organic Letters, 2022, 24, 1491-1495.	4.6	6
5	Preparation and characterization of lignin grafted layered double hydroxides for sustainable service of bitumen under ultraviolet light. Journal of Cleaner Production, 2022, 350, 131536.	9.3	12
6	Regio- and Enantioselective Hydroalkylations of Unactivated Olefins Enabled by Nickel Catalysis: Reaction Development and Mechanistic Insights. ACS Catalysis, 2022, 12, 5795-5805.	11.2	31
7	Highly Enantioselective Synthesis of [1,2,4]Triazino[5,4- <i>a</i> ]isoquinoline Derivatives via (3 + 3) Cycloaddition Reactions of Diazo Compounds and Isoquinolinium Methylides. Organic Letters, 2022, 24, 3766-3771.	4.6	7
8	The Collective Power of Genetically Encoded Protein/Peptide Tags and Bioorthogonal Chemistry in Biological Fluorescence Imaging. ChemPhotoChem, 2021, 5, 187-216.	3.0	6
9	Mechanistic insights into the rhodium–copper cascade catalyzed dual C–H annulation of indoles. Organic Chemistry Frontiers, 2021, 8, 1739-1746.	4.5	8
10	Combining palladium and ammonium halide catalysts for Morita–Baylis–Hillman carbonates of methyl vinyl ketone: from 1,4-carbodipoles to ion pairs. Chemical Science, 2021, 12, 11399-11405.	7.4	20
11	A ratiometric fluorescent probe for monitoring pH fluctuations during autophagy in living cells. Chemical Communications, 2021, 57, 1510-1513.	4.1	37
12	Hydroxyaromatic Fluorophores. ACS Omega, 2021, 6, 3447-3462.	3.5	7
13	How Solvents Control the Chemoselectivity in Rh-Catalyzed Defluorinated [4 + 1] Annulation. Organic Letters, 2021, 23, 1489-1494.	4.6	10
14	Synergistic Dinuclear Rhodium Induced Rhodium-Walking Enabling Alkene Terminal Arylation: A Theoretical Study. ACS Catalysis, 2021, 11, 3975-3987.	11.2	11
15	Cellulosic Cul Nanoparticles as a Heterogeneous, Recyclable Catalyst for the Borylation of α,β-Unsaturated Acceptors in Aqueous Media. Catalysis Letters, 2021, 151, 3220-3229.	2.6	7
16	Revealing HOCl burst from endoplasmic reticulum in cisplatin-treated cells via a ratiometric fluorescent probe. Chinese Chemical Letters, 2021, 32, 1795-1798.	9.0	53
17	Visible-Light-Driven Anti-Markovnikov Hydrocarboxylation of Acrylates and Styrenes with CO <sub>2</sub> . CCS Chemistry, 2021, 3, 1746-1756.	7.8	70
18	Palladium-Catalyzed Modular and Enantioselective <i>cis</i> -Difunctionalization of 1,3-Enynes with Imines and Boronic Reagents. Journal of the American Chemical Society, 2021, 143, 17989-17994.	13.7	37

#	Article	IF	CITATIONS
19	Cu <sup>II</sup> â€Catalyzed Oxidative Formation of 5â€Alkynyltriazoles. Chemistry - an Asian Journal, 2020, 15, 380-390.	3.3	4
20	Nucleophilicity versus BrĄ̃nsted Basicity Controlled Chemoselectivity: Mechanistic Insight into Silver- or Scandium-Catalyzed Diazo Functionalization. ACS Catalysis, 2020, 10, 1256-1263.	11.2	31
21	A novel benzothiazine-fused coumarin derivative for sensing hypochlorite with high performance. Dyes and Pigments, 2020, 182, 108675.	3.7	28
22	Visibleâ€Light Photoredoxâ€Catalyzed Remote Difunctionalizing Carboxylation of Unactivated Alkenes with CO <sub>2</sub> . Angewandte Chemie, 2020, 132, 21307-21314.	2.0	21
23	σ-Bond Migration Assisted Decarboxylative Activation of Vinylene Carbonate in Rh-Catalyzed 4 + 2 Annulation: A Theoretical Study. Organometallics, 2020, 39, 2813-2819.	2.3	19
24	Catalytic enantioselective construction of vicinal quaternary carbon stereocenters. Chemical Science, 2020, 11, 9341-9365.	7.4	96
25	Visibleâ€Light Photoredox atalyzed Remote Difunctionalizing Carboxylation of Unactivated Alkenes with CO <sub>2</sub> . Angewandte Chemie - International Edition, 2020, 59, 21121-21128.	13.8	102
26	Nickel-catalyzed migratory alkyl–alkyl cross-coupling reaction. Chemical Science, 2020, 11, 10461-10464.	7.4	20
27	The influence of amino substituents on the signalâ€output, selectivity, and sensitivity of a hydroxyaromatic 1,2,3â€triazolyl chemosensor for anions—A structure–property relationship investigation. Journal of Physical Organic Chemistry, 2020, 33, e4078.	1.9	3
28	SNAP/CLIP-Tags and Strain-Promoted Azide–Alkyne Cycloaddition (SPAAC)/Inverse Electron Demand Diels–Alder (IEDDA) for Intracellular Orthogonal/Bioorthogonal Labeling. Bioconjugate Chemistry, 2020, 31, 1370-1381.	3.6	26
29	Kinetically Controlled Radical Addition/Elimination Cascade: From Alkynyl Aziridine to Fluorinated Allenes. Organic Letters, 2020, 22, 2419-2424.	4.6	16
30	Protecting-Group-Free Total Syntheses of (±)-Norascyronones A and B. Organic Letters, 2020, 22, 2517-2521.	4.6	13
31	Layered Chirality Relay Model in Rh(I)-Mediated Enantioselective C–Si Bond Activation: A Theoretical Study. Organic Letters, 2020, 22, 2124-2128.	4.6	23
32	Expanding the substrate selectivity of SNAP/CLIP-tagging of intracellular targets. Methods in Enzymology, 2020, 638, 233-257.	1.0	3
33	Enantiodivergence by minimal modification of an acyclic chiral secondary aminocatalyst. Nature Communications, 2019, 10, 5182.	12.8	35
34	Highly Selective and Catalytic Generation of Acyclic Quaternary Carbon Stereocenters via Functionalization of 1,3-Dienes with CO <sub>2</sub> . Journal of the American Chemical Society, 2019, 141, 18825-18835.	13.7	104
35	Oxidative Addition Promoted C–C Bond Cleavage in Rh-Mediated Cyclopropenone Activation: A DFT Study. ACS Catalysis, 2019, 9, 10876-10886.	11.2	40
36	Unmasking the Ligand Effect in Manganese-Catalyzed Hydrogenation: Mechanistic Insight and Catalytic Application. Journal of the American Chemical Society, 2019, 141, 17337-17349.	13.7	102

#	Article	IF	CITATIONS
37	Formal Asymmetric Cycloaddition of Activated α,β-Unsaturated Ketones with α-Diazomethylphosphonate Mediated by a Chiral Silver SPINOL Phosphate Catalyst. Organic Letters, 2019, 21, 593-597.	4.6	22
38	Mechanistic Insight into Palladiumâ€Catalyzed Carbocyclizationâ€Functionalization of Bisallene: A Computational Study. ChemCatChem, 2019, 11, 1228-1237.	3.7	20
39	An unusual [4 + 2] fusion strategy to forge meso-N/O-heteroarene-fused (quinoidal) porphyrins with intense near-infrared Q-bands. Chemical Science, 2019, 10, 7274-7280.	7.4	20
40	Theoretical prediction on the reactivity of the Co-mediated intramolecular Pauson-Khand reaction for constructing bicyclo-skeletons in natural products. Chinese Chemical Letters, 2019, 30, 889-894.	9.0	13
41	Theoretical Study of the Addition of Cu–Carbenes to Acetylenes to Form Chiral Allenes. Journal of the American Chemical Society, 2019, 141, 5772-5780.	13.7	35
42	Theoretical study of FMO adjusted C-H cleavage and oxidative addition in nickel catalysed C-H arylation. Communications Chemistry, 2019, 2, .	4.5	12
43	Site-Selective α-Alkoxyl Alkynation of Alkyl Esters Mediated by Boryl Radicals. Organic Letters, 2019, 21, 2927-2931.	4.6	16
44	Asymmetric Propargylic Radical Cyanation Enabled by Dual Organophotoredox and Copper Catalysis. Journal of the American Chemical Society, 2019, 141, 6167-6172.	13.7	174
45	Unveiling how intramolecular stacking modes of covalently linked dimers dictate photoswitching properties. Nature Communications, 2019, 10, 5480.	12.8	6
46	Acyl radical to rhodacycle addition and cyclization relay to access butterfly flavylium fluorophores. Nature Communications, 2019, 10, 5664.	12.8	9
47	Well-Designed Phosphine–Urea Ligand for Highly Diastereo- and Enantioselective 1,3-Dipolar Cycloaddition of Methacrylonitrile: A Combined Experimental and Theoretical Study. Journal of the American Chemical Society, 2019, 141, 961-971.	13.7	70
48	Theoretical Advances on the Mechanism of Transition Metal-Catalyzed C—F Functionalization. Chinese Journal of Organic Chemistry, 2019, 39, 38.	1.3	9
49	Pyrrole β-amides: Synthesis and characterization of a dipyrrinone carboxylic acid and an N-Confused fluorescent dipyrrinone. Tetrahedron, 2018, 74, 1698-1704.	1.9	4
50	Fluorescence of Hydroxyphenyl-Substituted "Click―Triazoles. Journal of Physical Chemistry A, 2018, 122, 2956-2973.	2.5	21
51	Synthesis of 1-Cyanoalkynes and Their Ruthenium(II)-Catalyzed Cycloaddition with Organic Azides to Afford 4-Cyano-1,2,3-triazoles. Journal of Organic Chemistry, 2018, 83, 5092-5103.	3.2	20
52	Ruthenium(II)â€Catalyzed Câ^'H Difluoromethylation of Ketoximes: Tuning the Regioselectivity from the <i>meta</i> to the <i>para</i> Position. Angewandte Chemie, 2018, 130, 1291-1295.	2.0	26
53	Ruthenium-catalyzed umpolung carboxylation of hydrazones with CO <sub>2</sub> . Chemical Science, 2018, 9, 4873-4878.	7.4	62
54	Ruthenium(II)-enabled para-selective C–H difluoromethylation of anilidesÂand their derivatives. Nature Communications, 2018, 9, 1189.	12.8	104

#	Article	IF	CITATIONS
55	Theoretical insight into phosphoric acid-catalyzed asymmetric conjugate addition of indolizines to α,β-unsaturated ketones. Chinese Chemical Letters, 2018, 29, 1237-1241.	9.0	26
56	Insights into disilylation and distannation: sequence influence and ligand/steric effects on Pd-catalyzed difunctionalization of carbenes. Dalton Transactions, 2018, 47, 1819-1826.	3.3	21
57	Ruthenium(II)â€Catalyzed Câ^'H Difluoromethylation of Ketoximes: Tuning the Regioselectivity from the <i>meta</i> to the <i>para</i> Position. Angewandte Chemie - International Edition, 2018, 57, 1277-1281.	13.8	100
58	The mechanism of copper-catalyzed oxytrifluoromethylation of allylamines with CO <sub>2</sub> : a computational study. Organic Chemistry Frontiers, 2018, 5, 633-639.	4.5	46
59	Retro-metal-ene <i>versus</i> retro-Aldol: mechanistic insight into Rh-catalysed formal [3+2] cycloaddition. Chemical Communications, 2018, 54, 13551-13554.	4.1	4
60	Beyond O <sup>6</sup> -Benzylguanine: O <sup>6</sup> -(5-Pyridylmethyl)guanine as a Substrate for the Self-Labeling Enzyme SNAP-Tag. Bioconjugate Chemistry, 2018, 29, 4104-4109.	3.6	9
61	Excitation-Dependent Multiple Fluorescence of a Substituted 2-(2′-Hydroxyphenyl)benzoxazole. Journal of Physical Chemistry A, 2018, 122, 9209-9223.	2.5	30
62	Mechanistic Insights into Manganese (I) atalyzed Chemoselective Hydroarylations of Alkynes: A Theoretical Study. ChemCatChem, 2018, 10, 5280-5286.	3.7	12
63	Mechanistic view of Ru-catalyzed C–H bond activation and functionalization: computational advances. Chemical Society Reviews, 2018, 47, 7552-7576.	38.1	212
64	Annulation cascade of arylnitriles with alkynes to stable delocalized PAH carbocations <i>via</i> intramolecular rhodium migration. Chemical Science, 2018, 9, 5488-5493.	7.4	34
65	Experimental and Theoretical Studies on Ru(II)-Catalyzed Oxidative C–H/C–H Coupling of Phenols with Aromatic Amides Using Air as Oxidant: Scope, Synthetic Applications, and Mechanistic Insights. ACS Catalysis, 2018, 8, 8324-8335.	11.2	34
66	Borylation of α,β-Unsaturated Acceptors by Chitosan Composite Film Supported Copper Nanoparticles. Nanomaterials, 2018, 8, 326.	4.1	9
67	Recyclable Heterogeneous Chitosan Supported Copper Catalyst for Silyl Conjugate Addition to α,β-Unsaturated Acceptors in Water. Polymers, 2018, 10, 385.	4.5	12
68	Catalytic Lactonization of Unactivated Aryl C–H Bonds with CO <sub>2</sub> : Experimental and Computational Investigation. Organic Letters, 2018, 20, 3776-3779.	4.6	64
69	Thiolate–palladium( <scp>iv</scp> ) or sulfonium–palladate(0)? A theoretical study on the mechanism of palladium-catalyzed C–S bond formation reactions. Organic Chemistry Frontiers, 2017, 4, 943-950.	4.5	13
70	Enantioselective alkynylation of N-sulfonyl α-ketiminoesters via a Friedel–Crafts alkylation strategy. Chemical Communications, 2017, 53, 5890-5893.	4.1	20
71	Bioinspired Total Synthesis of Homodimericinâ€A. Angewandte Chemie, 2017, 129, 7998-8002.	2.0	4
72	Bioinspired Total Synthesis of Homodimericinâ€A. Angewandte Chemie - International Edition, 2017, 56, 7890-7894.	13.8	25

#	Article	IF	CITATIONS
73	lr(III)/Ir(V) or Ir(I)/Ir(III) Catalytic Cycle? Steric-Effect-Controlled Mechanism for the <i>para</i> -C–H Borylation of Arenes. Organometallics, 2017, 36, 2107-2115.	2.3	38
74	Bioinspired Asymmetric Synthesis of Hispidaninâ€A. Angewandte Chemie - International Edition, 2017, 56, 5844-5848.	13.8	24
75	Bioinspired Asymmetric Synthesis of Hispidaninâ€A. Angewandte Chemie, 2017, 129, 5938-5942.	2.0	3
76	Stabilization of Two Radicals with One Metal: A Stepwise Coupling Model for Copper-Catalyzed Radical–Radical Cross-Coupling. Scientific Reports, 2017, 7, 43579.	3.3	35
77	Highly enantioselective nitro-Mannich reaction of ketimines under phase-transfer catalysis. Organic Chemistry Frontiers, 2017, 4, 1266-1271.	4.5	33
78	Progressive structural modification to a zinc-actuated photoinduced electron transfer (PeT) switch in the context of intracellular zinc imaging. Organic and Biomolecular Chemistry, 2017, 15, 9139-9148.	2.8	5
79	Rhodium/Copper Cocatalyzed Highly trans-Selective 1,2-Diheteroarylation of Alkynes with Azoles via C–H Addition/Oxidative Cross-Coupling: A Combined Experimental and Theoretical Study. Journal of the American Chemical Society, 2017, 139, 15724-15737.	13.7	59
80	From Mechanistic Study to Chiral Catalyst Optimization: Theoretical Insight into Binaphthophosphepine-catalyzed Asymmetric Intramolecular [3 + 2] Cycloaddition. Scientific Reports, 2017, 7, 7619.	3.3	11
81	Radical Trifluoromethylative Dearomatization of Indoles and Furans with CO <sub>2</sub> . ACS Catalysis, 2017, 7, 8324-8330.	11.2	85
82	Reactivity and regioselectivity in Diels–Alder reactions of anion encapsulated fullerenes. Physical Chemistry Chemical Physics, 2017, 19, 30393-30401.	2.8	19
83	Ligand effect on nickle-catalyzed reductive alkyne-aldehyde coupling reactions: a computational study. Scientia Sinica Chimica, 2017, 47, 341-349.	0.4	2
84	Structural Determinants of Alkyne Reactivity in Copper-Catalyzed Azide-Alkyne Cycloadditions. Molecules, 2016, 21, 1697.	3.8	23
85	Frontispiece: Efficient Synthesis of Dimeric Oxazoles, Piperidines and Tetrahydroisoquinolines from <i>N</i> â€Substituted 2â€Oxazolones. Chemistry - A European Journal, 2016, 22, .	3.3	0
86	Efficient Synthesis of Dimeric Oxazoles, Piperidines and Tetrahydroisoquinolines from <i>N</i> ‣ubstituted 2â€Oxazolones. Chemistry - A European Journal, 2016, 22, 7696-7701.	3.3	11
87	On the Mechanism of Copper(I)-Catalyzed Azide-Alkyne Cycloaddition. Chemical Record, 2016, 16, 1501-1517.	5.8	74
88	Zinc(II) Complexes of N , N â€Di(2â€picolyl)hydrazones. European Journal of Inorganic Chemistry, 2016, 2016, 5477-5484.	2.0	3
89	Dual Role of Acetate in Copper(II) Acetate Catalyzed Dehydrogenation of Chelating Aromatic Secondary Amines: A Kinetic Case Study of Copper atalyzed Oxidation Reactions. European Journal of Inorganic Chemistry, 2016, 2016, 3728-3743.	2.0	18
90	Cu(II)-Catalyzed Oxidative Formation of 5,5′-Bistriazoles. Journal of Organic Chemistry, 2016, 81, 12091-12105.	3.2	32

#	Article	IF	CITATIONS
91	Mechanism of Synergistic Cu(II)/Cu(I)-Mediated Alkyne Coupling: Dinuclear 1,2-Reductive Elimination after Minimum Energy Crossing Point. Journal of Organic Chemistry, 2016, 81, 1654-1660.	3.2	42
92	Rhodium-Catalyzed Hetero-(5 + 2) Cycloaddition of Vinylaziridines and Alkynes: A Theoretical View of the Mechanism and Chirality Transfer. Organometallics, 2016, 35, 771-777.	2.3	33
93	Titelbild: Precise Design of Phosphorescent Molecular Butterflies with Tunable Photoinduced Structural Change and Dual Emission (Angew. Chem. 33/2015). Angewandte Chemie, 2015, 127, 9553-9553.	2.0	Ο
94	Inside Back Cover: Fabrication of Highly Stable Glycoâ€Gold Nanoparticles and Development of a Glycoâ€Gold Nanoparticleâ€Based Oriented Immobilized Antibody Microarray for Lectin (GOAL) Assay (Chem. Eur. J. 10/2015). Chemistry - A European Journal, 2015, 21, 4163-4163.	3.3	1
95	Tuning the Reactivity of Radical through a Triplet Diradical Cu(II) Intermediate in Radical Oxidative Cross-Coupling. Scientific Reports, 2015, 5, 15934.	3.3	34
96	Precise Design of Phosphorescent Molecular Butterflies with Tunable Photoinduced Structural Change and Dual Emission. Angewandte Chemie - International Edition, 2015, 54, 9591-9595.	13.8	85
97	Development of a Rhodium(II)â€Catalyzed Chemoselective C(sp <sup>3</sup> )H Oxygenation. Chemistry - A European Journal, 2015, 21, 14937-14942.	3.3	38
98	5-Arylvinylene-2,2′-bipyridyls: Bright "push–pull―dyes as components in fluorescent indicators for zinc ions. Journal of Photochemistry and Photobiology A: Chemistry, 2015, 311, 1-15.	3.9	46
99	Enhancing the Photostability of Arylvinylenebipyridyl Compounds as Fluorescent Indicators for Intracellular Zinc(II) Ions. Journal of Organic Chemistry, 2015, 80, 5600-5610.	3.2	17
100	Silver Migration Facilitates Isocyanide-Alkyne [3 + 2] Cycloaddition Reactions: Combined Experimental and Theoretical Study. ACS Catalysis, 2015, 5, 6640-6647.	11.2	66
101	Mechanism of Copper(I)-Catalyzed 5-Iodo-1,2,3-triazole Formation from Azide and Terminal Alkyne. Journal of Organic Chemistry, 2015, 80, 9542-9551.	3.2	41
102	Absorption and Emission Sensitivity of 2â€(2′â€Hydroxyphenyl)benzoxazole to Solvents and Impurities. Photochemistry and Photobiology, 2015, 91, 586-598.	2.5	26
103	A Fluorescent Indicator for Imaging Lysosomal Zinc(II) with Förster Resonance Energy Transfer (FRET)â€Enhanced Photostability and a Narrow Band of Emission. Chemistry - A European Journal, 2015, 21, 867-874.	3.3	48
104	Bis[ <i>N</i> -alkyl- <i>NN</i> -di(2-pyridylmethyl)amine]zinc(II) perchlorates display <i>cis-facial</i> stereochemistry in solid state and solution. Supramolecular Chemistry, 2014, 26, 214-222.	1.2	14
105	A Phosphorescent Molecular "Butterfly―that undergoes a Photoinduced Structural Change allowing Temperature Sensing and White Emission. Angewandte Chemie - International Edition, 2014, 53, 10908-10912.	13.8	129
106	Distinguishing Förster resonance energy transfer and solvent-mediated charge-transfer relaxation dynamics in a zinc(ii) indicator: a femtosecond time-resolved transient absorption spectroscopic study. Physical Chemistry Chemical Physics, 2014, 16, 5088-5092.	2.8	7
107	Zn( <scp>ii</scp> )-coordination modulated ligand photophysical processes – the development of fluorescent indicators for imaging biological Zn( <scp>ii</scp> ) ions. RSC Advances, 2014, 4, 20398-20440.	3.6	99
108	Fused Polycyclic Compounds via Cycloaddition of 4-(1′-Cyclohexenyl)-5-iodo-1,2,3-triazoles with 4-Phenyl-1,2,4-triazoline-3,5-dione: The Importance of a Sacrificial Iodide Leaving Group. Journal of Organic Chemistry, 2013, 78, 5038-5044.	3.2	10

#	Article	IF	CITATIONS
109	Integrated and Passive 1,2,3-Triazolyl Groups in Fluorescent Indicators for Zinc(II) Ions: Thermodynamic and Kinetic Evaluations. Inorganic Chemistry, 2013, 52, 5838-5850.	4.0	67
110	Synthesis of 5-lodo-1,2,3-triazoles from Organic Azides and Terminal AlkynesÂ <del>:</del> Ligand Acceleration Effect, Substrate Scope, and Mechanistic Insights. Synthesis, 2013, 45, 2372-2386.	2.3	33
111	Tricolor Emission of a Fluorescent Heteroditopic Ligand over a Concentration Gradient of Zinc(II) Ions. Journal of Organic Chemistry, 2012, 77, 8268-8279.	3.2	51
112	Tunable Dual Fluorescence of 3â€(2,2′â€Bipyridyl)â€Substituted Iminocoumarin. ChemPhysChem, 2012, 13, 3827-3835.	2.1	18
113	Structurally Diverse Copper(II) Complexes of Polyaza Ligands Containing 1,2,3-Triazoles: Site Selectivity and Magnetic Properties. Inorganic Chemistry, 2012, 51, 3465-3477.	4.0	78
114	Zn <sup>II</sup> and Pb <sup>II</sup> coordination chemistry of 2,6-bis(1,2,3-triazol-4-yl)pyridine (clickate) and the metal ion-dependent emission of â€~clickate'–appended anthracene. Supramolecular Chemistry, 2012, 24, 696-706.	1.2	14
115	Chemoselective Sequential "Click―Ligation Using Unsymmetrical Bisazides. Organic Letters, 2012, 14, 2590-2593.	4.6	61
116	Synthesis of 5-lodo-1,4-disubstituted-1,2,3-triazoles Mediated by in Situ Generated Copper(I) Catalyst and Electrophilic Triiodide Ion. Journal of Organic Chemistry, 2012, 77, 6443-6455.	3.2	116
117	Experimental Investigation on the Mechanism of Chelation-Assisted, Copper(II) Acetate-Accelerated Azide–Alkyne Cycloaddition. Journal of the American Chemical Society, 2011, 133, 13984-14001.	13.7	160
118	Balance between Fluorescence Enhancement and Association Affinity in Fluorescent Heteroditopic Indicators for Imaging Zinc Ion in Living Cells. Inorganic Chemistry, 2011, 50, 10493-10504.	4.0	25
119	A FRET-based indicator for imaging mitochondrial zinc ions. Chemical Communications, 2011, 47, 11730.	4.1	77
120	Tridentate complexes of 2,6-bis(4-substituted-1,2,3-triazol-1-ylmethyl)pyridine and its organic azide precursors: an application of the copper(ii) acetate-accelerated azide–alkyne cycloaddition. Dalton Transactions, 2011, 40, 3655.	3.3	46
121	Ligandâ€Assisted, Copper(II) Acetateâ€Accelerated Azide–Alkyne Cycloaddition. Chemistry - an Asian Journal, 2011, 6, 2825-2834.	3.3	46
122	Chelation-Assisted, Copper(II)-Acetate-Accelerated Azideâ^'Alkyne Cycloaddition. Journal of Organic Chemistry, 2010, 75, 6540-6548.	3.2	146
123	2-Anthryltriazolyl-Containing Multidentate Ligands: Zinc-Coordination Mediated Photophysical Processes and Potential in Live-Cell Imaging Applications. Inorganic Chemistry, 2010, 49, 4278-4287.	4.0	66
124	Electronic structural dependence of the photophysical properties of fluorescent heteroditopic ligands – implications in designing molecular fluorescent indicators. Organic and Biomolecular Chemistry, 2010, 8, 5431.	2.8	16
125	Metal-coordination-mediated sequential chelation-enhanced fluorescence (CHEF) and fluorescence resonance energy transfer (FRET) in a heteroditopic ligand system. New Journal of Chemistry, 2010, 34, 2176.	2.8	41
126	Mini review: Fluorescent heteroditopic ligands of metal ions. Supramolecular Chemistry, 2009, 21, 268-283.	1.2	26

#	Article	IF	CITATIONS
127	Structures, Metal Ion Affinities, and Fluorescence Properties of Soluble Derivatives of Tris((6-phenyl-2-pyridyl)methyl)amine. Inorganic Chemistry, 2009, 48, 11196-11208.	4.0	16
128	Catechol boronate formation and its electrochemical oxidation. Chemical Communications, 2009, , 2151.	4.1	29
129	Apparent Copper(II)-Accelerated Azideâ^'Alkyne Cycloaddition. Organic Letters, 2009, 11, 4954-4957.	4.6	198
130	Fluorescence of 5-Arylvinyl-5′-Methyl-2,2′-Bipyridyl Ligands and Their Zinc Complexes. Journal of Organic Chemistry, 2009, 74, 8761-8772.	3.2	51
131	A fluorescent heteroditopic ligand responding to free zinc ion over six orders of magnitude concentration range. Chemical Communications, 2009, , 7408.	4.1	22
132	A Heteroditopic Fluoroionophoric Platform for Constructing Fluorescent Probes with Large Dynamic Ranges for Zinc Ions. Chemistry - A European Journal, 2008, 14, 2894-2903.	3.3	85
133	Unimolecular binary half-adders with orthogonal chemical inputs. Chemical Communications, 2008, , 1880.	4.1	22
134	Photochemically Stable Fluorescent Heteroditopic Ligands for Zinc Ion. Journal of Organic Chemistry, 2008, 73, 8321-8330.	3.2	41
135	Fluorescent dyes of the esculetin and alizarin families respond to zinc ions ratiometrically. Chemical Communications, 2007, , 1891.	4.1	66
136	Highly Sensitive Fluorescent Probes for Zinc Ion Based on Triazolyl-Containing Tetradentate Coordination Motifs. Organic Letters, 2007, 9, 4999-5002.	4.6	188
137	Two Methods for the Determination of Enantiomeric Excess and Concentration of a Chiral Sample with a Single Spectroscopic Measurement. Chemistry - A European Journal, 2007, 13, 99-104.	3.3	50
138	A Structural Investigation of the Nâ^'B Interaction in ano-(N,N-Dialkylaminomethyl)arylboronate System. Journal of the American Chemical Society, 2006, 128, 1222-1232.	13.7	306
139	Signal Amplification by Allosteric Catalysis. Angewandte Chemie - International Edition, 2006, 45, 1190-1196.	13.8	139
140	Guidelines in Implementing Enantioselective Indicator-Displacement Assays for α-Hydroxycarboxylates and Diols. Journal of the American Chemical Society, 2005, 127, 4260-4269.	13.7	175
141	FRET induced by an â€~allosteric' cycloaddition reaction regulated with exogenous inhibitor and effectors. Tetrahedron, 2004, 60, 7267-7275.	1.9	50
142	Facile Quantification of Enantiomeric ExcessandConcentration with Indicator-Displacement Assays:Â An Example in the Analyses of α-Hydroxyacids. Journal of the American Chemical Society, 2004, 126, 3676-3677.	13.7	212
143	Geometry-Dependent Phosphodiester Hydrolysis Catalyzed by Binuclear Copper Complexes. Inorganic Chemistry, 2003, 42, 7912-7920.	4.0	81
144	Nylon/DNA:Â Single-Stranded DNA with a Covalently Stitched Nylon Lining. Journal of the American Chemical Society, 2003, 125, 10178-10179.	13.7	55

#	Article	IF	CITATIONS
145	REACTION OF N3-BENZOYL-3â€ <sup>2</sup> ,5â€ <sup>2</sup> -O-(DI-TERT-BUTYLSILANEDIYL)URIDINE WITH HINDERED ELECTROPHILES: INTERMOLECULAR N3To 2â€ <sup>2</sup> -OPROTECTING GROUP TRANSFER. Nucleosides, Nucleotides and Nucleic Acids, 2002, 21, 723-735.	1.1	9
146	Copper(II)-Catalyzed 1,6-Hydroboration Reactions of p‑Quinone Methides Under Ligand-Free Conditions: A Sequential Methodology to gem-Disubstituted Methanols. Catalysis Letters, 0, , .	2.6	1